

# Direct and Selective Synthesis of a Wide Range of Carbon Nanomaterials by CVD at CMOS Compatible Temperatures

Irene Taurino<sup>\*\*1</sup>, Arnaud Magrez<sup>2</sup>, László Forró<sup>3</sup>, Giovanni De Micheli<sup>1</sup>, *Member, IEEE*,  
and Sandro Carrara<sup>1</sup>, *Member, IEEE*

**Abstract**—Biosensors benefit from specific nano-structuration of the active bio-interface layer. In this perspective, a wide range of carbon nanomaterials including multi-walled carbon nanotubes (MWCNTs), nanographite and carbon nanowalls (CNWs) have been directly synthesised by chemical vapor deposition (CVD) on Pt microelectrodes for the first time down to CMOS-compatible temperatures. This integration process, extremely useful to develop nanostructured multi-sensing site biodevices, has been validated by testing sensors for glucose with enhanced and competitive performance. Moreover it paves the way to the full integration of CMOS circuits, nanostructures and bioprobes.

**Keywords**—multi-site biosensors, carbon nanomaterials, CVD, CMOS-compatible temperatures

## I. INTRODUCTION

**F**AST and simultaneous monitoring of many metabolites is an urgent need in fields as medicine, environment and food analysis. In particular, the demand for a rapid and accurate multi-sensing technology is essential for clinicians. The availability of devices that provide the exact concentration of a set of metabolites in real-time favours faster and more appropriate both therapeutic or diagnostic interventions. Theoretically, instrumentation designed for a timely multi-sensing should be able to do several measurements from a small volume and undiluted sample. Consequently, the development of a tiny device is a crucial requirement.

Compared with the historically used analytical techniques (e. g. chromatography, spectrophotometry), the electrochemical detection offers many advantages including high sensitivities, simple use, in situ and continuous monitoring, low cost. The possibility to integrate electrochemical sensors onto simple and portable instrumentation is due to their easy miniaturisation. Interestingly sensors based on miniaturised electrochemical cells have shown remarkable sensitivity and reproducibility when applied

to monitor human metabolites [1], [2]. Moreover, small electrodes allow us to design many sensing sites, each one specific for one metabolite, onto a tiny platform creating a multipanel device. Such a kind of sensor is very useful for personalised medicine [3] and possible subcutaneous implantations [4], [5]. The compatibility of their fabrication with the low-cost CMOS technology is extremely useful to implement a full parallel process.

To further improve detection performance, carbon nanomaterials are considered due to their high electrocatalytic activity, large surface area and good support for enzyme immobilisation [6]. Many efforts have been made to integrate carbon nanomaterials onto CMOS-sensors [7], [8], [9]. In particular, metal microelectrodes are historically modified with carbon nanostructures by time-consuming, expensive and hardly-reproducible techniques. Additives (e.g. polymers [10]), commonly employed to help the nanostructuration step, inevitably mask the nanomaterials promising properties and compromise the time-stability of the device due to the binder-matrix instability in aqueous environments. A realistic approach to enable a close coupling of only nanomaterials and electrodes is the direct CVD growth on CMOS wafers. Advantages of the CVD technology are (i) the no post-growth processing (ii) the easy scalability to wafer size and (iii) the well-established presence in the semiconductor industry. In our previous work, we have already succeeded in the not trivial growth of carbon nanomaterials on metal microelectrodes [11]. However, the process was performed at high growth temperatures (600-750 °C) that are not compatible with conventional CMOS processes. These temperatures cause irreversible material stresses that inevitably compromise the normal operation of the device with on-board electronic components. To make the whole process compatible with the electronics, the upper limit growth temperature is 450 °C [12]. Recently, many efforts have been made to lower the synthesis temperatures for fabricating graphitic nanomaterials. However, in the majority of cases, nanomaterials are grown on insulating substrates, on which the effectiveness of the catalyst is more pronounced. Nessim *et. al.* have already reported the CNT synthesis on metals at CMOS compatible temperatures by thermal decomposition of the hydrocarbon/hydrogen gas mixture. The nanofabrication consisted of only CNTs and was carried out on Pd and Ta in a non-selective way. Indeed, in biosensing,

<sup>1</sup> Laboratory of Integrated Systems, EPFL, Lausanne, Switzerland

<sup>2</sup> Crystal Growth Facility, EPFL, Lausanne, Switzerland

<sup>3</sup> Laboratory of Physics of Complex Matter, EPFL, Lausanne, Switzerland

<sup>\*\*</sup> Contacting Author: EPFL IC ISIM LS11 INF 334 (Btiment INF)  
Station 14 CH-1015 Lausanne E-mail: irene.taurino@epfl.ch; Fax: +41  
21 69 34 225; Tel: +41 21 69 38168

we need to address specific sites of a platform commonly made of Au and Pt [13].

In the present study, we describe a versatile process to integrate a wide range of carbon nanomaterials onto an array of Pt working electrodes of a biosensor by a CVD process down to 450 °C. We successfully satisfied the three major requirements for an effective integration of nanocarbon into microelectrochemical biosystems: 1. Selectivity with respect to one working electrode (WE) made of Pt of a multi-sensing platform 2. intimate coupling nanomaterials-electrodes avoiding the use of additional materials. 3. synthesis at CMOS compatible temperatures opening the possibility of a direct integration nanostructures/front-end CMOS data acquisition circuits. Finally, glucose detection, performed by incorporating the glucose oxidase (GODx) as probe-enzyme onto the nanostructured microelectrodes, has shown excellent sensing parameters proving the efficiency of the proposed nanointegration approach in biosensing applications.

## II. MATERIALS AND METHODS

### A. Catalyst electrodeposition and nanocarbon synthesis

Fe<sub>2</sub>Co nanoparticles (NPs) were deposited by a voltammetric method, while chronoamperometry was used to deposit compact Fe<sub>2</sub>Co layers from Fe and Co sulphate solutions.

After the catalyst electrodeposition, the devices were firstly placed in the furnace already at the growth temperature and kept there for 10 minutes under H<sub>2</sub> and Ar flow (60 l/h). Then, Ar was introduced at 45 l/h together with C<sub>2</sub>H<sub>2</sub> and CO<sub>2</sub> (ratio: 1:1; flow: 0.25 l/h) for 5 minutes at a temperature ranging between 600 °C and 450 °C. Then, the chamber was cleaned under Ar flow (60 l/h) for 10 minutes [11]. Before the measurements, a chemical activation (6 hours in sulphuric acid 6 M) was carried out to increase the electron transfer from the nanostructures [14] and to make the surface more hydrophilic for an easier incorporation of enzymes [15].

### B. Chemicals and apparatus

Cobalt(II) and iron(II) sulfate heptahydrate were purchased from AppliChem. All metal solutions contained 0.5 M boric acid (AppliChem) and 0.5 M sodium chloride (Sigma). Sulphuric acid from Merck was used for the nanomaterial activation. The glucose detection was carried out by casting 1 μl of glucose oxidase (25 mg/ml, Roche in 2.5% glutaraldehyde) onto a nanostructured microelectrode and kept overnight before any measurement. The concentration of D-glucose (Sigma) was increased by steps of 100 μM up to 500 μM and of 250 μM up to 4.5 mM. Phosphate buffer saline (10 mM PBS, pH 7.4, Sigma) was employed for the amperometric measurements (applied potential: +650 mV) by using an Autolab potentiostat controlled by Nova software. Enzyme-electrodes were stored at 4 °C under dry conditions. Scanning electron microscope (SEM)

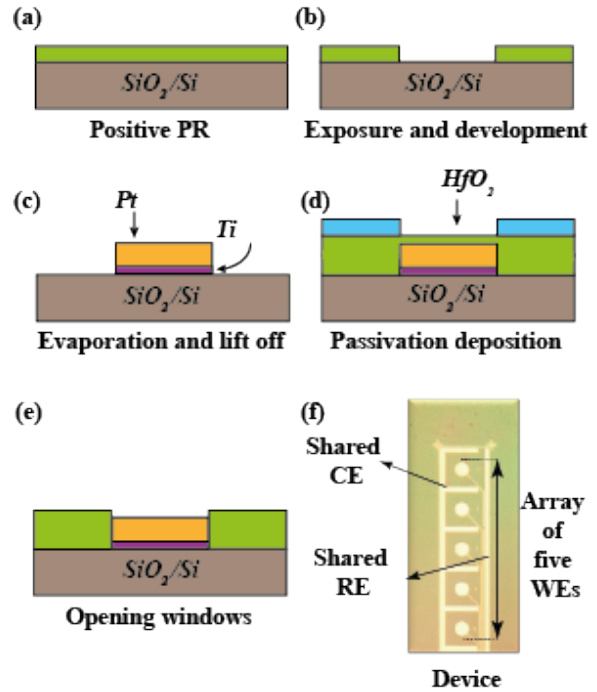


Fig. 1. Schematic of the device microfabrication.

images were recorded with a Zeiss MERLIN SEM. The MWCNT diameter was calculated with an ImageJ software [16]. Filtering and analysis of the data were realised using Igor Pro software (Wavemetrics, Lake Oswego, OR, USA).

## III. RESULTS AND DISCUSSION

### A. Multi-sensing platform fabrication

The main steps of the device fabrication are shown in Fig. 1. Briefly, we used positive photoresist on Si wafers with 500 nm of native SiO<sub>2</sub> (Fig. 1 (a)). Platinum (200 nm) was deposited by evaporation (Alcatel EVA 600). A buffer layer of Ti (20 nm) was added to improve the adhesion between Pt and SiO<sub>2</sub> (Fig. 1 (b) and (c)). After the lift-off, 20 nm of HfO<sub>2</sub> were deposited via atomic layer deposition (BENEQ TFS200) (Fig. 1 (d)). Afterwards, microelectrodes and contacts were introduced on the dielectric material. HfO<sub>2</sub> was selectively removed by dry etching (Alcatel AMS 200 DSE) (Fig. 1 (e)). Then, a wafer dicing step produced single devices each one with five working electrodes (diameter of 564 μm). All the working electrodes share the same counter and reference electrode (Fig. 1 (f)). HfO<sub>2</sub> was selected as passivation layer for its excellent adhesion to the bottom layers at the growth temperatures. CNTs tend to spontaneously grow onto insulating materials without any predeposited catalyst. To avoid not selective growths, the synthesis time was reduced till no CNTs were seen onto the surface of HfO<sub>2</sub>.

### B. Catalyst electrodeposition

Electrodeposition was employed as novel, low-cost, versatile and selective technique, even compatible with

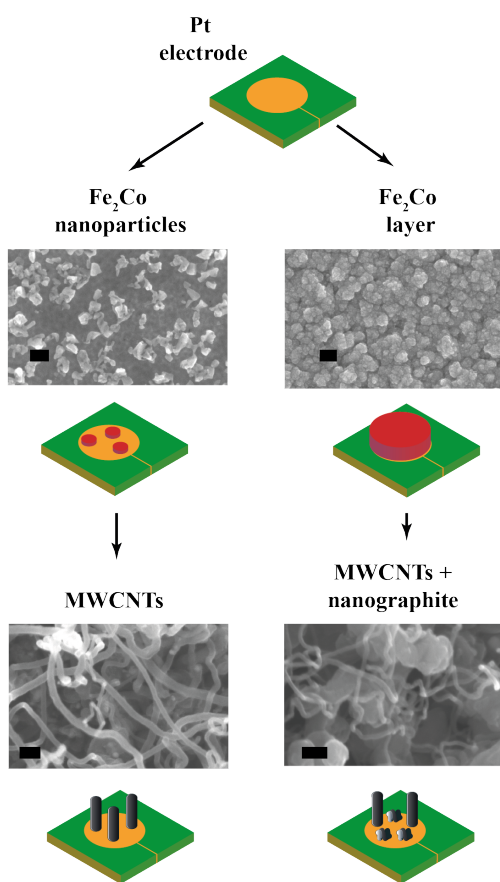


Fig. 2. Schematic of the carbon nanomaterial CVD growth from catalyst nanoparticles (on the left) and from catalyst compact layers (on the right). Black bars: 100 nm.

the platform, to easily obtain different catalyst coatings. Carbon nanomaterials have been previously synthesised from Fe predeposited onto Pt electrodes at temperatures ranging from 600 °C to 750 °C. Below 600 °C, Fe on Pt was catalytically inactive. The maximum nanocarbon yield for the CVD system we utilised has been previously obtained for Fe/Co alloy in a molar ratio 2:1 [17]. The electrodeposition of  $\text{Fe}_2\text{Co}$  was optimised for both catalyst nanoparticles and coatings.  $\text{Fe}_2\text{Co}$  nanoparticles resulted from solutions with equimolar concentrations of the two metals (average molar ratio:  $2.15 \pm 0.11$ ). On the other hand,  $\text{Fe}_2\text{Co}$  coatings have been obtained by from sulphate solutions of iron and cobalt in a molar ratio 2:1 (average molar ratio from coatings with different thicknesses is  $2.12 \pm 0.05$ ). The morphology of  $\text{Fe}_2\text{Co}$  nanoparticles and layers is shown in Fig. 2. Fig. 3 clearly shows the increase of the nanocarbon yield when the alloy is used as catalyst material (carbon nanomaterials grown on Fe (a) and on  $\text{Fe}_2\text{Co}$  (b) nanoparticles).

### C. Growths down to CMOS compatible temperatures

*a) Synthesis from catalyst nanoparticles:* We obtained sparse rolls of MWCNTs (Fig. 2 and Fig. 4 (a))

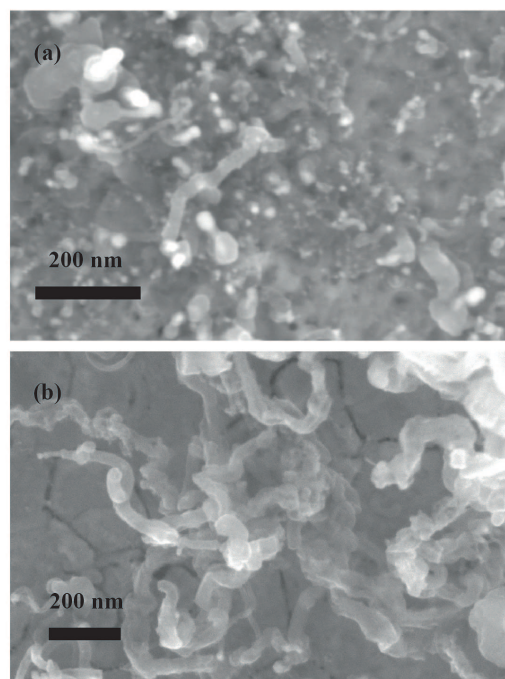


Fig. 3. Increase of the nanocarbon yield passing from Fe (a) to  $\text{Fe}_2\text{Co}$  (b) as catalyst.

with an average diameter equal to  $(34.4 \pm 19.4)$  nm using  $\text{Fe}_2\text{Co}$  nanoparticles. Longer, denser and larger MWCNTs (average diameter:  $(52.7 \pm 22.6)$  nm) with intercalated nanographite were observed by triplicating the deposition time (from 5 to 15 minutes; Fig. 4 (b) and (c)). Fig. 5 shows that a narrow diameter distribution results from a lower synthesis temperature. In addition, the average diameter decreases going down with the temperature (from  $(34.4 \pm 19.4)$  nm at 600 °C to  $(26.5 \pm 6.5)$  nm at 450 °C). No nanocarbon deposits were obtained at temperature lower than 450 °C.

*b) Synthesis from catalyst coatings:* Fig. 6 shows the nanocarbon deposits resulting from catalyst coatings with increased thickness. Larger MWCNTs (Fig. 6 (a)) were obtained passing from 2 s to 4 s of deposited catalyst. Nanofibers were grown from thicker layers (8 s of catalyst deposition). From 15 s of electrodeposited  $\text{Fe}_2\text{Co}$ , hybrid nanographite/MWCNTs were produced (Fig. 2 and Fig. 6 (b)). Only nanographite was synthesised from even thicker catalyst coatings (Fig. 6 (c)). The average MWCNT/CNF diameter versus the deposition time is shown in Fig. 6 (d). Once nanographite starts to grow the MWCNT diameter drastically decreases.

We carried out different depositions at temperatures lower than 600 °C from  $\text{Fe}_2\text{Co}$  coatings. Nanographite was obtained from thinner  $\text{Fe}_2\text{Co}$  coatings than using higher temperatures (Fig. 7 (a) and (b)). Also at lower

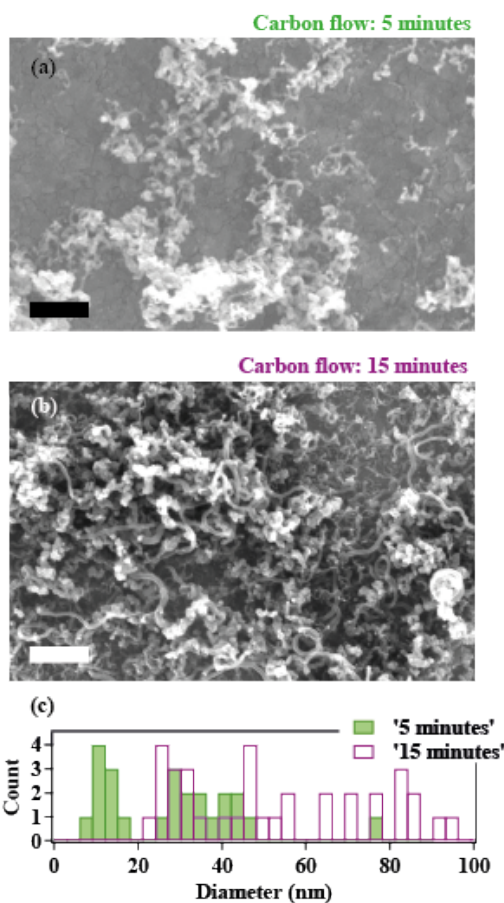


Fig. 4. SEM images of carbon nanomaterials fabricated on catalyst nanoparticles at 600 °C under 5 (a) and 15 (b) minutes of carbon flow. Bars: 1  $\mu\text{m}$ . (c) Diameter distribution of MWCNTs produced under two different growth times: 5 (green bars) and 15 (purple bars) minutes.

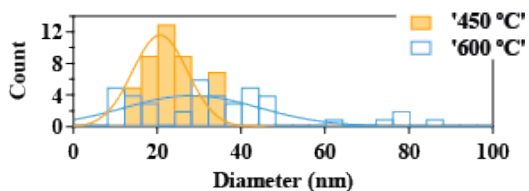


Fig. 5. Diameter distribution of MWCNTs grown from  $\text{Fe}_2\text{Co}$  nanoparticles at 600 °C (blue) and at 450 °C (yellow).

temperatures, the synthesis of nanographite determines a simultaneous reduction of the CNT diameter (Fig. 7 (c)). Thicker catalyst layers were not catalytically active at 450 °C.

*c) Implementing two successive growths:* The highest is the nanocarbon yield, the greater is the augment of electroactive area so an enhanced electrochemical response is expected. In addition, a bigger surface area favours both incorporation and stabilisation of biomacromolecules. The last point is of crucial importance for enzyme-mediated detection mechanisms. With this nanofabrication approach, the reduction of the temperature produces a considerable

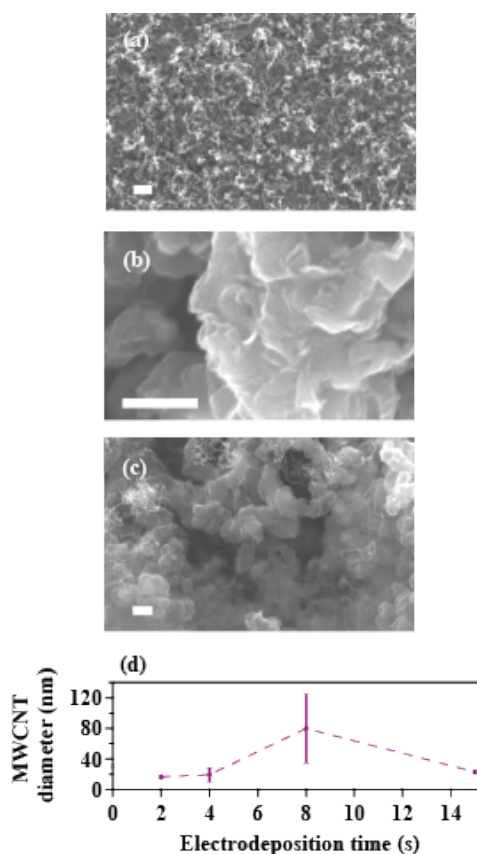


Fig. 6. SEM images of MWCNTs grown on 2 s (a) of electrodeposited catalyst coating. SEM images of hybrid MWCNTs-nanographite (b) and nanographite (c) produced on 15 s and 30 s of deposited  $\text{Fe}_2\text{Co}$  coatings. Effect of the  $\text{Fe}_2\text{Co}$  electrodeposition time on the nanotube/nanofiber diameter (e). White bars: 200 nm.

drop in the nanocarbon yield. To increase the yield of the nanostructures, we carried out two successive depositions at 450 °C. After the first synthesis, we deposited thin layers of  $\text{Fe}_2\text{Co}$  on the top of nanomaterials grown at the first stage (Fig. 8 (a)). After, a second synthesis was carried out keeping identical growth parameters. From 2 s of electrodeposited catalyst we obtained more carbon nanomaterials, namely CNWs with intercalated MWCNTs (Fig. 8 (b)). Electrodeposition of  $\text{Fe}_2\text{Co}$  for 4 s results in an increase of the CNT quantity (Fig. 8 (c)). Also amorphous carbon grows when the catalyst is electrodeposited for a longer interval time.

#### D. Application for glucose measurements

The device with the nanostructured working microelectrodes has been tested for sensing glucose, whose detection was performed by incorporating a glucose oxidase as probe-enzyme onto the electrodes. The morphological change of our nanostructures proves the enzyme incorporation (Fig. 9 (a) and (b)). Glucose oxidase was adsorbed onto the nanomaterials and crosslinked with glutaraldehyde. The sensor was linear up to 1 mM (Fig. 9 (c) and



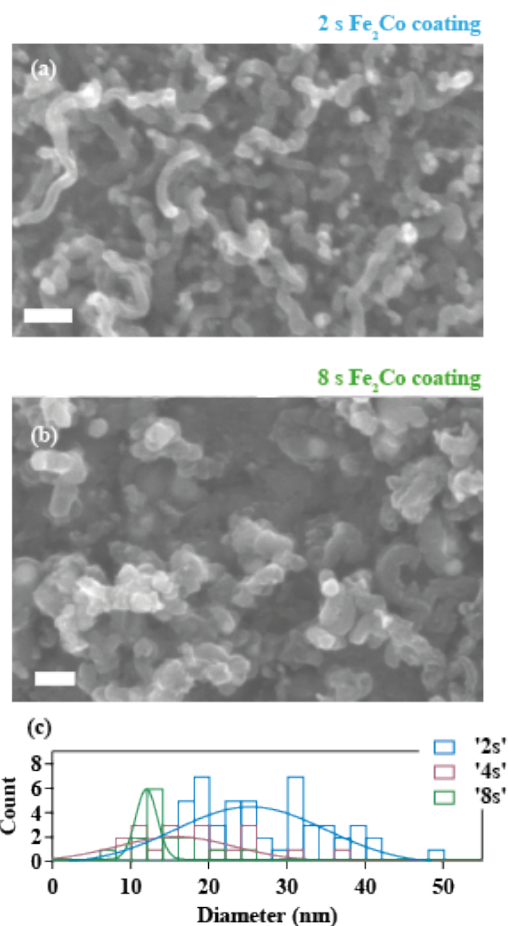


Fig. 7. SEM images of nanomaterials produced at 525 °C on 2 s (a) and 8 s (b) of deposited catalyst layers. (c) Diameter distribution of MWCNTs grown on three different Fe<sub>2</sub>Co coatings at 450 °C. White bars: 100 nm.

(d)). Sensitivity and LOD were  $70.4 \pm 0.3 \mu\text{A}/(\text{mM cm}^2)$  and  $5.0 \pm 3.3 \mu\text{M}$ , respectively. The enzyme-based sensor shows competitive performance if compared with those reported in literature [15]. Glutaraldehyde was utilised to prolong the time-stability of the enzyme. Sensitivity decreases of about 35% and LOD did not vary after three days following the protein immobilisation. Five days after the enzyme immobilisation, the protein lost its activity toward the glucose detection.

#### IV. CONCLUSIONS

Carbon nanomaterials are typically synthesised *via* CVD at 650-1200 °C, temperatures not compatible with a direct CMOS integration. Here, for the first time, we report a method to obtain MWCNTs, nanographite and CNWs down to 450 °C, opening the possibility to a direct integration nanostructures/front-end of CMOS data acquisition circuits. We succeeded in growths on only the selected metal WEs of a multi-panel biosensing-platform avoiding the co-immobilisation of additional binders. Furthermore, we easily obtained different kinds of carbon nanostructures only by changing the nature of the electrodeposited

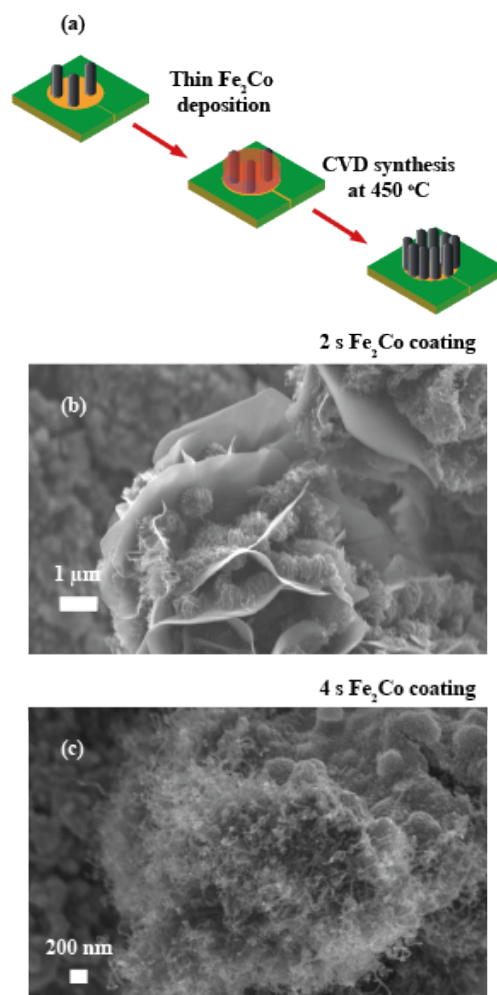


Fig. 8. Two deposition CVD process (a); CNWs and MWCNTs grown onto 2 s of electrodeposited Fe<sub>2</sub>Co (b); MWCNTs grown onto 4 s of electrodeposited Fe<sub>2</sub>Co (c).

catalyst thanks to the high versatility of our approach. We succeeded in increasing the nanocarbon yield at 450 °C that is of crucial importance for high performance biodetection. Finally, the described integration method was proven to be robust and highly efficient for oxidase-mediated amperometric sensing of glucose.

#### ACKNOWLEDGMENT

The authors would like to thank Andrea Cavallini for the design of the microfabricated platform and Laurent Bernard for the preparation of the CVD system. The research was supported by the i-IronIC++ and ERC NanoSys projects. Arnaud Magrez acknowledges financial support from the SCOPES project n °IZ74Z0 137458 and the European project NAMASEN.

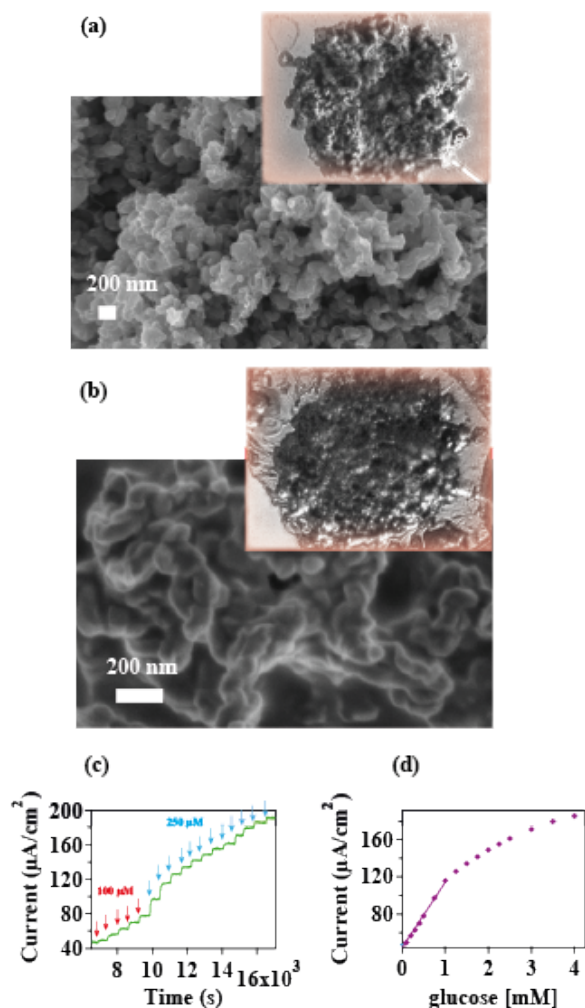


Fig. 9. Optical and SEM images of the nanostructured electrode before (a) and after (b) the protein incorporation. Chronoamperometry (c) and calibration curve (d) of the glucose micro-nanosensor.

## REFERENCES

- [1] I. Moser, G. Jobst, and G. A. Urban, "Biosensor arrays for simultaneous measurement of glucose, lactate, glutamate, and glutamine," *Biosensors and Bioelectronics*, vol. 17, no. 4, pp. 297–302, 2002.
- [2] M. Miyashita, N. Ito, S. Ikeda, T. Murayama, K. Oguma, and J. Kimura, "Development of urine glucose meter based on micro-planer amperometric biosensor and its clinical application for self-monitoring of urine glucose," *Biosensors and Bioelectronics*, vol. 24, no. 5, pp. 1336–1340, 2009.
- [3] S. Carrara, A. Cavallini, V. Erokhin, and G. De Micheli, "Multi-panel drugs detection in human serum for personalized therapy," *Biosensors and Bioelectronics*, vol. 26, no. 9, pp. 3914–3919, 2011.
- [4] S. Carrara, S. Ghoreishizadeh, J. Olivo, I. Taurino, C. Baj-Rossi, A. Cavallini, M. Op de Beeck, C. Dehollain, W. Bursleson, F. G. Moussy *et al.*, "Fully integrated biochip platforms for advanced healthcare," *Sensors*, vol. 12, no. 8, pp. 11 013–11 060, 2012.
- [5] S. Carrara, A. Cavallini, S. Ghoreishizadeh, J. Olivo, and G. De Micheli, "Developing highly-integrated subcutaneous biochips for remote monitoring of human metabolism," in *IEEE Sensors conference*, 2012, pp. 28–31.
- [6] W. Yang, K. R. Ratinac, S. P. Ringer, P. Thordarson, J. J. Gooding, and F. Braet, "Carbon nanomaterials in biosensors: should you use nanotubes or graphene?" *Angewandte Chemie International Edition*, vol. 49, no. 12, pp. 2114–2138, 2010.
- [7] C. T. Chow, M. L. Sin, P. H. Leong, W. J. Li, and K. Pun, "Design and modeling of a cnt-cmos low-power sensor chip," in *Nano/Micro Engineered and Molecular Systems, 2007. NEMS'07. 2nd IEEE International Conference on*. IEEE, 2007, pp. 1209–1214.
- [8] R. S. Chakraborty, S. Narasimhan, and S. Bhunia, "Hybridization of cmos with cnt-based nano-electromechanical switch for low leakage and robust circuit design," *Circuits and Systems I: Regular Papers, IEEE Transactions on*, vol. 54, no. 11, pp. 2480–2488, 2007.
- [9] Y. Zhou, J. L. Johnson, A. Ural, and H. Xie, "Localized growth of carbon nanotubes on cmos substrate at room temperature using maskless post-cmos processing," *Nanotechnology, IEEE Transactions on*, vol. 11, no. 1, pp. 16–20, 2012.
- [10] J. Wang, M. Musameh, and Y. Lin, "Solubilization of carbon nanotubes by Nafion toward the preparation of amperometric biosensors," *Journal of the American Chemical Society*, vol. 125, no. 9, pp. 2408–2409, 2003.
- [11] I. Taurino, A. Magrez, F. Matteini, L. Forró, G. De Micheli, and S. Carrara, "Direct growth of nanotubes and graphene nanoflowers on electrochemical platinum electrodes," *Nanoscale*, vol. 5, no. 24, pp. 12 448–12 455, 2013.
- [12] V. T. Renard, M. Jublot, P. Gergaud, P. Cherno, D. Rouchon, A. Chabli, and V. Jousseume, "Catalyst preparation for CMOS-compatible silicon nanowire synthesis," *Nature nanotechnology*, vol. 4, no. 10, pp. 654–657, 2009.
- [13] J. Shen and C.-C. Liu, "Development of a screen-printed cholesterol biosensor: Comparing the performance of gold and platinum as the working electrode material and fabrication using a self-assembly approach," *Sensors and Actuators B: Chemical*, vol. 120, no. 2, pp. 417–425, 2007.
- [14] M. Pumera, T. Sasaki, and H. Iwai, "Relationship between carbon nanotube structure and electrochemical behavior: heterogeneous electron transfer at electrochemically activated carbon nanotubes," *Chemistry—An Asian Journal*, vol. 3, no. 12, pp. 2046–2055, 2008.
- [15] Y. Chen, J. Huang, and C. Chuang, "Glucose biosensor based on multiwalled carbon nanotubes grown directly on Si," *Carbon*, vol. 47, no. 13, pp. 3106–3112, 2009.
- [16] W. Rasband, "ImageJ," *U. S. National Institutes of Health, Bethesda, Maryland, USA, 1997–2011*, <http://imagej.nih.gov/ij/>.
- [17] A. Magrez, J. Seo, R. Smajda, B. Korbely, J. Andresen, M. Mionić, S. Casimirius, and L. Forró, "Low-temperature, highly efficient growth of carbon nanotubes on functional materials by an oxidative dehydrogenation reaction," *ACS Nano*, vol. 4, no. 7, pp. 3702–3708, 2010.